Check for
updates

Optically reconfigurable non-reciprocal bistable absorption based on one-dimensional photonic crystal of plasma and non-linear materials

Yi Xu[1] · Baofei Wan[1] · Ziwei Zhou[1] · Haifeng Zhang[1,2,3] · Dan Zhang[2]

Abstract

In this article, a one-dimensional asymmetric photonic crystal (PC) structure based on the magnetized and non-magnetized plasma and non-linear materials is designed, and the features of the PCs are simulated and analyzed by the transfer matrix method. We realize the optical reconfigurable bistable (ORB) absorption of one-dimensional PCs and discover that due to the asymmetry of the spatial structure distribution and the magneto-optical effect of the plasma when the light is incident from the front or back direction, and the absorption characteristics have obvious non-reciprocity. The most noteworthy is that when the light incidents from two different directions, the bistable threshold interval position and size have changed significantly. Compared with the forward incidence, when the light is incident from the backward direction, the ORB threshold increases, and a significant left shift occurs. We further discussed the influences of the frequency of the magnetized plasma and angle in different incident directions on the results of bistable absorption, and give an analysis of the reflection and transmission results under the same conditions.

1 Introduction

Photonic crystals (PCs) are artificial optical materials composed of media with different refractive indexes arranged in a certain periodic sequence and are important materials for the development of a new generation of optoelectronic information technology [1, 2]. The photonic band gap (PBG) and local state are their unique properties, which can effectively control the propagation of electromagnetic waves [3, 4]. The introduction of different defects in the PCs will cause the change of the PBGs, resulting in different optical effects, which makes the PCs be used in the preparation of many high-performance photonic devices [5, 6]. Plasma is a macroscopically electrically neutral ionized body [7]. Its internal

particle movement is restricted by electromagnetic field forces and can interact with electromagnetic fields [8–10]. Plasma is introduced into the PCs as a special defect, and the adjustable control of electromagnetic wave (EW) propagation in different bands can be achieved by changing the plasma density, temperature, and other related parameters [11, 12]. In addition, the interaction between incident EW and ions will increase as the plasma frequency and collision frequency increase, and energy transfer occurs, resulting in a certain absorption bandwidth [13, 14]. Therefore, the plasma PCs can be used in absorbers [15]. In recent years, non-linear optics also has become a hot research topic due to its advantages in performance, response speed, and processability [15, 16]. Optical bistability (OB) is one of the important research directions. OB means that an input light intensity has two stable output light intensity states that can be converted to each other [17, 18]. Bistable systems can be used to design optical switches, optical storage, and other optical devices.

With the innovation of related technologies such as information processing, transmission, and storage, researchers are paying more and more attention to the research of the two major sectors of plasma and nonlinearity. Ma et al. [19] theoretically studied a one-dimensional PC composed of an air layer, magnetized and non-magnetized plasma, and analyzed

✉ Haifeng Zhang
  hanlor@163.com

1 College of Electronic and Optical Engineering and College of Microelectronics, Nanjing University of Posts and Telecommunications, Nanjing 210023, China

2 College of Information Science and Technology, Nanjing Forestry University, Nanjing 210037, China

3 State Key Laboratory of Millimeter Waves of Southeast University, Nanjing 210096, China

using the transfer matrix method to realize the forward ultra-wideband absorption and reverse polarization splitting. It opens up a new way for reconfigurable one-way applications. Reflection and transmission properties of one-dimensional plasma/polystyrene non-linear PCs have been investigated theoretically by Kumar et al. [20], they calculated the reflectance and transmission intensity of EWs when the control waves of different intensities passed through this periodic multilayer structure, and the reflectance of the structure can be changed by adjusting the intensity of the control waves was found. Kong et al. [21] designed a structure composed of non-linear plasma and metamaterials alternately. The non-reciprocal absorption characteristics are realized through the coupling of evanescent and propagating waves in the asymmetric structure. And the absorption and reflection of the bistable state are implemented by the introduction of non-linear materials. This provided a certain theoretical basis for the new omnidirectional EW absorber. It can be seen that many researchers have been involved in the research on the structure of the combination of plasma and non-linear materials, and the non-reciprocal absorption characteristics controlled by light stress have also been brought about, but they are all concentrated on the unidirectional absorption level. There is little discussion about the non-reciprocal two-way absorption of forward and backward.

In this paper, a PC structure composed of magnetized and non-magnetized plasma, non-linear dielectric layers, and ordinary dielectric layers is put forward, and the transmission matrix method is used to analyze the absorption characteristics for light waves of this structure. It can be found that this structure can achieve optically reconfigurable bistable (ORB) absorption. When the light is incident from the forward and backward directions, the non-linear absorption spectrum will also change significantly. When the light is incident in the forward direction, the bistable threshold is very small, and when the light is incident from the backward, the bistable threshold interval increases significantly, a Kenspeckle left shift has occurred, and an absorption zero point has appeared. After that, we further discussed the influences of angle and frequency of magnetized plasma on the non-reciprocal bistable absorption characteristics and found that the structure is more

sensitive to changes in the angle and magnetic field. Finally, the analysis of reflection and transmission spectra at small angles is also given. These findings can provide a new idea for the production of optical sensors, absorbers, and other devices. As a theoretical research paper, the experimental verification is not the content of this article.

2 Structure design and simulation

Figure 1 shows the structure diagram of the novel one-dimensional PCs we designed, which can be expressed as (AP1)9(CP2B)(P1A)8. The entire structure is exposed to the air. θ is the incident angle. A and B are ordinary dielectric layers, C is a non-linear material layer, and P1 and P2 are the non-magnetized and magnetized plasma layers. dA, dB, dC, $dP1$, and $dP2$ indicate the thicknesses of A, B, C, P1, and P2, respectively, where $dA = dB = dC = dP1 = dP2 = 0.1d$, and d is a constant. εi (i=A, B, C, P1, P2) describes the dielectric constant of A, B, C, P1, or P2 layer. To make the calculation of this structure applicable to any frequency, we normalized the frequency with $\omega 0$, and $\omega 0=2\pi c/d$.

The calculation of the plasma dielectric constant is different from that of conventional media. Next, we mainly take the TM wave as an example to give the calculation process of the plasma material [19, 22]. For the non-magnetized plasma

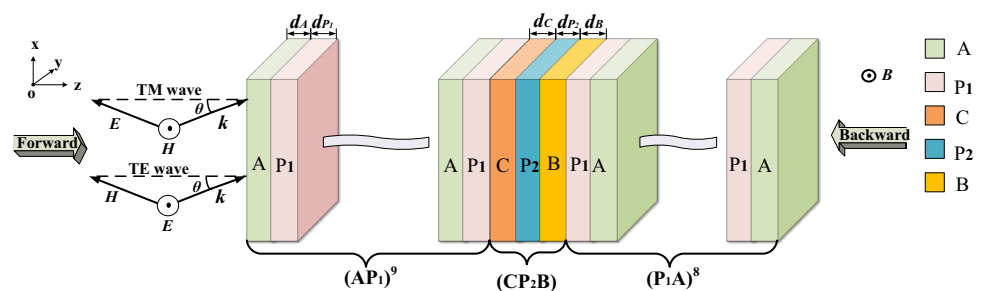$$\varepsilon_{p1} = 1 - \frac{\omega_{p1}^2}{\omega(\omega + iv_1)}, \tag{1}$$

where ω denotes the frequency of the incident wave, $\omega p1$ represents the non-magnetized plasma frequency, and $\nu 1$ is the collision frequency.

For the magnetized plasma

$$\varepsilon_{p2} = \frac{\varepsilon_1^2 - \varepsilon_2^2}{\varepsilon_1}, \tag{2}$$

where

Fig. 1 Schematic diagram of asymmetric 1D PCs' structure

$$\varepsilon_1 = 1 - \frac{\omega_{p2}^2(\omega + iv_2)}{\omega[(\omega + iv_2)^2 - \omega_{c2}^2]} \tag{3}$$

$$\varepsilon_2 = \frac{-\omega_{p2}^2\omega_{c2}}{\omega[(\omega + iv_2)^2 - \omega_{c2}^2]}, \tag{4}$$

where $\omega p2$ is the magnetized plasma frequency, $\omega c2$ describes the electron cyclotron frequency, and $\nu 2$ refers to the collision frequency. When the propagating wave is a TE wave, because the electric field of the TE wave is parallel to the applied magnetic field and is not affected by the magnetic field, and the expression of the dielectric constant of the magnetized plasma is consistent with that of the non-magnetized plasma, as shown in Eq. (1).

The transfer matrix of the magnetized plasma layer is as follows:

$$M_{p2} = \begin{bmatrix} \cos(k_{2z}d_{p2}) + \frac{k_{2x}\varepsilon_2}{k_{2z}\varepsilon_1}\sin(k_{1z}d_{p2}) & -\frac{i}{\eta_{p2}}\left[1 + \left(\frac{k_{2x}\varepsilon_2}{k_{2z}\varepsilon_1}\right)^2\right]\sin(k_{2z}d_{p2}) \\ -i\eta_{p2}\sin(k_{2z}d_{p2}) & \cos(k_{2z}d_{p2}) - \frac{k_{2x}\varepsilon_2}{k_{2z}\varepsilon_1}\sin(k_{2z}d_{p2}) \end{bmatrix}, \tag{5}$$

where $k2x = \omega/c \sqrt{\varepsilon_{p2}}\sin\theta_{p2}$, $k2z = \omega/c \sqrt{\varepsilon_{p2}}\cos\theta_{p2}$. $\eta p2 = \sqrt{\varepsilon_0/\mu_0}\sqrt{\varepsilon_{p2}}/\cos\theta_{p2}$.

The transmission matrices of the magnetized plasma for TE wave and the non-magnetized plasma layer are the same as that of the conventional medium, and the expression is

$$M_i = \begin{bmatrix} \cos\delta_i & -\frac{i}{\eta_i}\sin\delta_i \\ -i\eta_i\sin\delta_i & \cos\delta_i \end{bmatrix}, \tag{6}$$

where $\delta_i = (2\pi/\lambda)n_i d_i \cos\theta_i$, $\eta_i = n_i/\cos\theta_i$(TM wave) $\eta_i = n_i\cos\theta_i$(TE wave), $\theta_i = \arcsin(n_0\sin\theta_0/n_i)$, and n_i is refractive index of dielectric layer, $n_i = \varepsilon_i^{1/2}$.

Because of the particularity of non-linear materials, when the light passes through this material, its internal refractive index will be affected by the local field strength, so the transmission matrix of conventional media is not suitable for the non-linear media layers. Next, we give the calculation process of the non-linear material transfer matrix [21, 23].

The computing formula of the refractive index of the non-linear media layer is

$$n_c = n_l + \frac{\chi^{(3)}}{2n_l}|E|^2, \tag{7}$$

where nl signifies linear refractive index, $\chi(3)$ is third-order electrical polarization, and E indicates electric field strength in the dielectric layer. Its relationship with light intensity is as follows:

$$E = \sqrt{\frac{2I}{c\varepsilon_0}}. \tag{8}$$

The magnetic field strength

$$H = E\sqrt{\frac{\varepsilon_0}{\mu_0}}. \tag{9}$$

When calculating the transmission matrix of a non-linear dielectric layer, we can use limit and reverse thinking. If the non-linear medium layer is divided into enough sub-layers, so that each sub-layer is thin enough, the refractive index of the sub-layer can be regarded as not changing with the change of light intensity, and the transmission matrix of this sub-layer can then be calculated using Eq. (6). We assume that the non-linear medium is divided into q sub-layers, and q is plenty large. Take out the pth layer for analysis, there are

$$\begin{bmatrix} E_p \\ H_p \end{bmatrix} = M_p \begin{bmatrix} E_{p+1} \\ H_{p+1} \end{bmatrix}, \tag{10}$$

where Ep, $Ep+1$, Hp, $Hp+1$ represent the electric and magnetic field intensities at the light incident and emission boundaries of the pth layer, respectively. Where, using reverse thinking, assuming that the intensity of the emitted light is known, $Ep+1$ and $Hp+1$ can be solved according to the methods of Eqs. (8), (9), and (10). Mp is the transmission matrix of the pth sub-layer.

By analogy, we can get the light entrance and exit interfaces of the entire non-linear medium layer can be connected by

$$\begin{bmatrix} E_1 \\ H_1 \end{bmatrix} = M_1 M_2 \cdots M_p \cdots M_q \begin{bmatrix} E_{q+1} \\ H_{q+1} \end{bmatrix}. \tag{11}$$

That is, the transmission matrix of the non-linear medium layer is

$$M_C = M_1 M_2 \cdots M_p \cdots M_q. \tag{12}$$

The transfer matrix of the proposed structure can be described as

$$M = \left(M_A M_{P1}\right)^9 \left(M_C M_{P2} M_8\right) \left(M_{P1} M_A\right)^8 = \begin{pmatrix} m_{11} & m_{12} \\ m_{21} & m_{22} \end{pmatrix}. \tag{13}$$

After obtaining the transmission matrix, the reflection (r) and transmission (t) coefficients can be further calculated by the following formulas:

$$r = \frac{(m_{11} + m_{12}\eta_0)\eta_0 - (m_{21} + m_{22}\eta_0)}{(m_{11} + m_{12}\eta_0)\eta_0 + (m_{21} + m_{22}\eta_0)} \tag{14}$$

$$t = \frac{2\eta_0}{(m_{11} + m_{12}\eta_0)\eta_0 + (m_{21} + m_{22}\eta_0)}. \tag{15}$$

Reflectivity, transmittance, and absorptivity of the structure are

$$R = |r|^2, T = |t|^2, A = 1 - R - T \tag{16}$$

$$T = \frac{I_o}{I_i}, \tag{17}$$

where I_o and I_i represent the intensities of incoming and outgoing light, respectively.

3 Analysis and discussion

In this part of the simulation analysis where the incident wave is TM wave, the parameters we set are as follows: θ=0°, $\omega p1$=5$\omega 0$/6, $\omega p2$=4$\omega 0$, $\nu c1$=0.3$\omega p1$, $\nu c2$=0.003$\omega p2$, $\omega c2$=6$\omega p2$, $\chi^{(3)}$ =1.65×10–10 [24], εA=2, εB=3, and nl=2.75, respectively.

According to the parameters given above, we conducted a simulation analysis on the structure of this article, the irreversible bistable absorption contrast spectrum within a certain range of light intensity when the light passes through the structure is given, and its angular sensitivity and magnetized plasma frequency impact on results is discussed. At the same time, the non-reciprocal reflection and transmission characteristics and their angular sensitivity characteristics under the same conditions are also analyzed.

As shown in Fig. 2, due to the nonlinearity and loss characteristics of plasma and non-linear materials, the nonlinearity in the asymmetric structure is enhanced, resulting in the non-reciprocal bistable absorption of EWs. When the light is incident from the front direction, as the incident light intensity gradually increases, the absorption rate slowly decreases from the maximum value of 75%. When the light intensity builds up to 1.019 GW/m^2, the absorption rate has attenuated to 60.86%, and then falls to 28.73% as the light intensity increases. When the light intensity gradually goes down from a larger value, the jump-up point shifts to I_i=0.962 GW/m^2, and the absorption rate rises from 41.07 to 64.99%. When the light is incident from the backward direction, as the light intensity grows to 0.559 GW/m^2, the
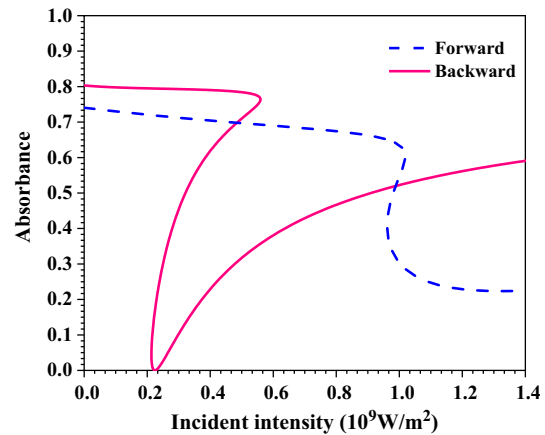

Fig. 2 Bistable absorption curves when the light is incident from the forward and backward directions

absorption rate decreases from 80.3 to 76.2%, and suddenly changes to 35.92%, and then increases in an upward trend. With the gradual decrease of light intensity, the absorption zero-point appears at 0.226 GW/m^2. When the light intensity goes down to the position of 0.214 GW/m^2 to the left of this point, the absorption rate will suddenly fall to 79.42%. Comparing the two curves, it can be obtained that when the light is coming from the front and back of the structure, the absorption curve has obvious non-reciprocity. The maximum value of the absorptance in the forward incident is lower than that in the backward incident, and the jump interval is obviously smaller and located at a larger light intensity. As a result, the reason which leads to the non-reciprocal bistable absorption, that is due to the asymmetry of the structure and the magneto-optic effect of the plasma.

The influences of the angle on the absorption curves are shown in Fig. 3. Figure 3a shows the case when the light comes from the backward. With the growth of angle, the maximums absorptivity aggrandizes slightly and the minimums clearly let up markedly. The jump-down points move a bit to the right, while the jump-up points move significantly to the left, and the bistable thresholds expand. When θ adds to 2°, 4°, and 6° in turn, the jump-up point of bistable absorption moves to 0.905, 0.814, and 0.652 GW/m^2, accordingly. And the corresponding absorption rates are 35.91%, 27.14%, and 11.91%. The minimum absorbance reduces to 18.72%, 12.78%, and 0. It can be seen that when the angle is 6°, the incident light intensity is 0.757 GW/m^2, an absorption zero-point occurs, and if the angle continues to magnify, a negative absorption rate will appear. When the light is incident on the forward, as shown in Fig. 3b, as the angle increases, both the maximum absorptance and the jump-down point decrease mildly, and the minimum absorptance and the jump-up point change more obviously. When θ starts from 0°, it increases to 6° by 2°, the upward
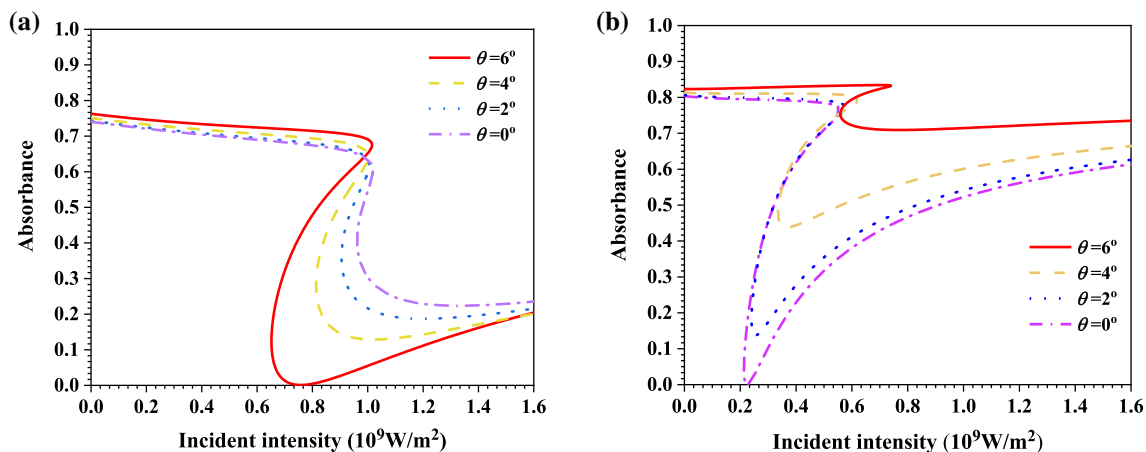
Fig. 3 The effects of angle ($\theta = 0°$, $2°$, $4°$, and $6°$) for the forward incidence (**a**) and the backward incidence (**b**) on the bistable absorption curves

jump point moves to 0.232, 0.337, and 0.555 GW/m², relatively, the corresponding absorption rates are 21.47%, 50.04%, and 75.45%, and the minimum values escalate to 13.74%, 43.85%, and 70.91%, respectively. According to the analysis of the pictures, the structure is extremely sensitive to the angle, and a small range of angle changes will have a distinct impact on the absorption curve.

From Eqs. (2) and (3), it can be seen that the change of the frequency of the magnetized plasma will cause the alter of its relative permittivity, and then cause the change of the refractive index, which will affect the absorption curve. As shown in Fig. 4a, b, the effects of the change in the frequency of magnetized plasma on the absorption curves when the light passes through the forward and backward are given. When ω_{p2} changes from $1.17\omega_0$ to $2\omega_0$ in the two figures, the changes in absorption curves are not evident. Observe Fig. 4a, when $\omega_{p2} = 4\omega_0$, as the light strength enhances, the absorption index starts to diminish tardily from 73.98%,

when $I_i = 0.946$ GW/m², the absorption index drops from 64.82 to 9.02%, and then relaxedly rises. With the light intensity transforms from large to small to 0.785 GW/m², the absorptivity will ascend from 25.39 to 67.56%. When $\omega_{p2} = 6\omega_0$, the downward jump point is located at 0.943 GW/m², and the absorptance has plunged from 68.79 to – 1.65%. The upward jump point is at 0.479 GW/m², and the absorptance raises from – 13.78 to 69.83%. Analyzing Fig. 4b, as ω_{p2} augments to $4\omega_0$ and $6\omega_0$, the jump-down point moves to the right to $I_i = 0.677$ and 0.974 GW/m², corresponding to the absorption rates of 78.26% and 50.12%, and the jump-up point shifts to the left, separately moving to 0.158 and 0.096 GW/m², the homologous absorption rates are -19.04% and -84.73%, and the bistable thresholds are visibly increased.

As shown in Fig. 4, the negative absorption rate can be achieved. For this phenomenon, the frequency-absorption index spectrum when the incident light intensity is 0.155
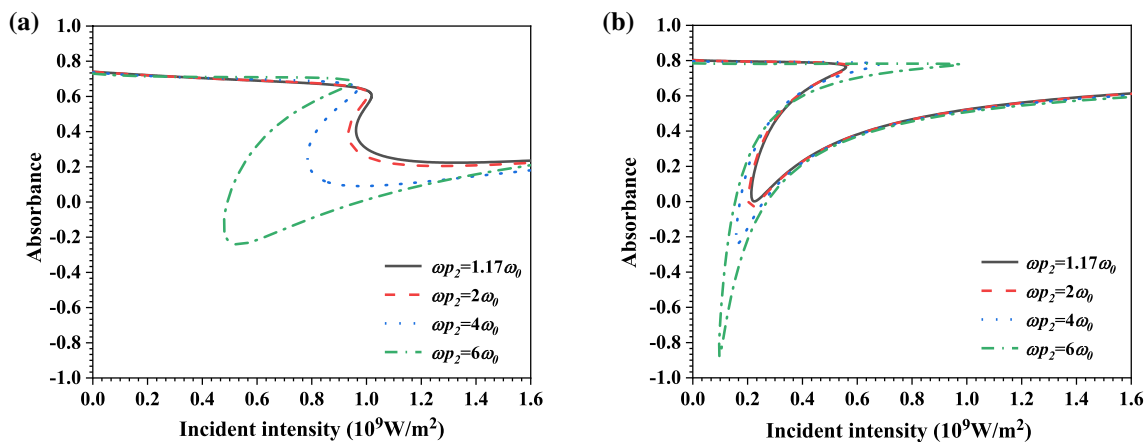

Fig. 4 The effects of $\omega_{p2} = 1.17\omega_0$, $2\omega_0$, $4\omega_0$, and $6\omega_0$ for the forward incidence (**a**) and the backward incidence (**b**) on the absorption bistable curves
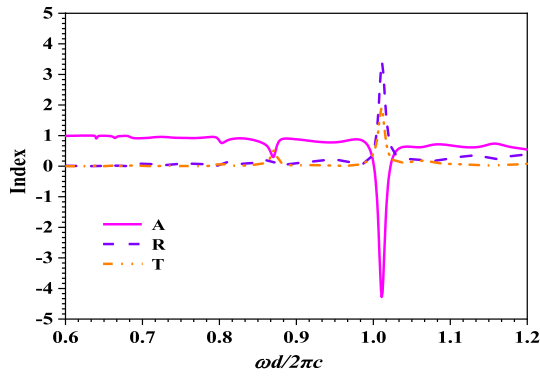
Fig. 5 The frequency-absorption spectrum of the lowest negative absorption point when $\omega p_2 = 6\omega_0$ for backward incident
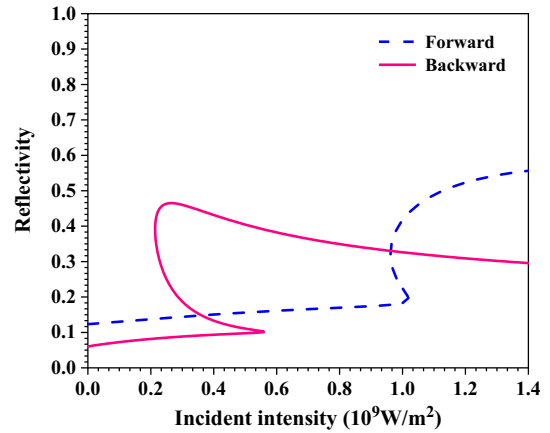

Fig. 6 The bistable transmission curves when the light is incident from the forward and backward directions
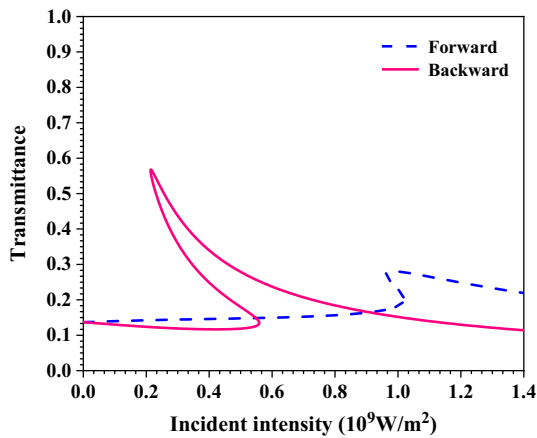

Fig. 8 The bistable reflection curves when the light is incident from the forward and backward directions

GW/m^2 is given in Fig. 5. It can be observed from Fig. 5 that the absorptivity is negative near $\omega d/2\pi c = 1$, and the reflectivity and transmittance are both greater than 1. Since the non-linear material acts as a non-linear gain medium here, when the incident light passes through the medium layer, an energy pumping effect will occur, which causes the light energy to be larger than the original incident light energy, which results in the above situation.

Figure 6 shows the transmission curve. When light is coming from the front, the transmittance elevates gradually with the growth of light intensity, increasing from 20.05% to 27.76% at $I_i = 1.019$ GW/m^2. When the light intensity starts to attenuate from a larger value, at $I_i = 0.952$ GW/m^2, the transmittance lowers from 27.41 to 17.18%. When the light inputs from the backward and gradually magnifies, the transmittance reduces and jumping from 13.26 to 25.08% at $I_i = 0.559$ GW/m^2. When the light intensity gradually declines from a larger value, the transmittance lets down
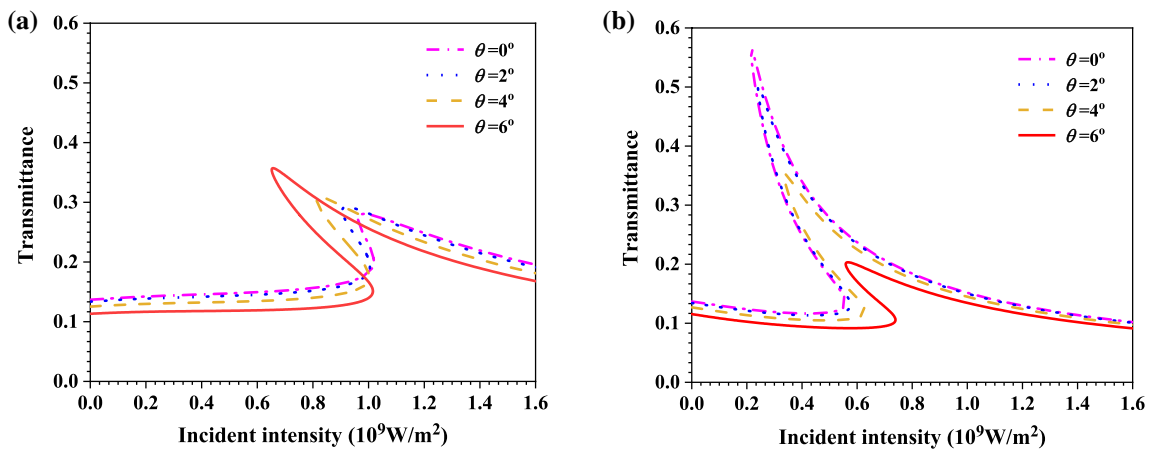

Fig. 7 The effects of angle ($\theta = 0°$, 2°, 4°, and 6°) for the forward incidence (**a**) and the backward incidence (**b**) on the bistable transmission curves
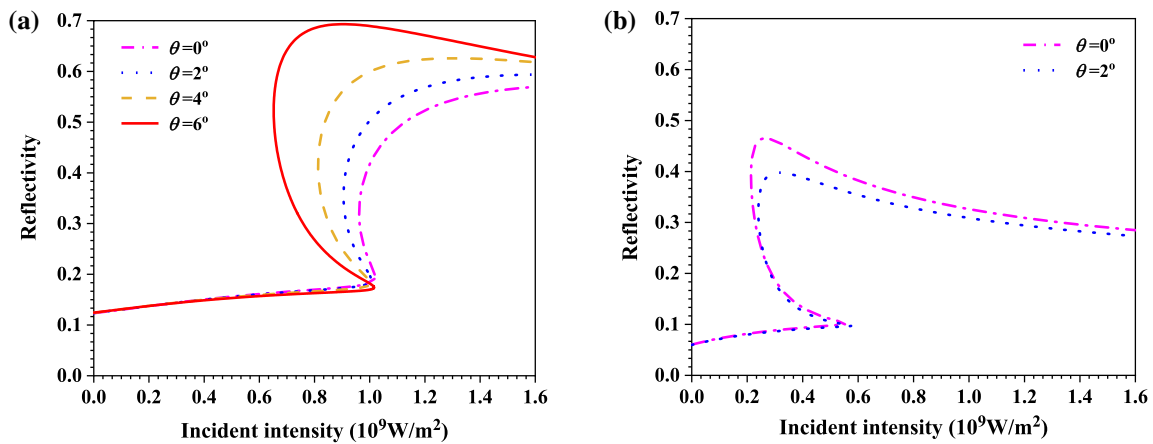
Fig. 9 The effects of angle ($\theta = 0°$, 2°, 4°, and 6°) for the forward incidence (**a**) and the backward incidence (**b**) on the bistable reflection curves

from 56.54 to 12.27% at $I_i = 0.214$ GW/m^2. Comparing the two curves, it can be seen that the bistable threshold district for the backward input is larger, and it is shifted to the left compared to the interval for the forward input, which is located in a smaller light intensity region.

As shown in Fig. 7a, when the light is incident on the forward, and the angle increases from 0° to 2°, the upward jump point does not change much, the downward jump point moves to the left to 0.916 GW/m^2, and the transmissivity will lower from 29.1 to 16.07% as the light intensity weakens. When $\theta = 4°$, the jump-up point is at $I_i = 1$ GW/m^2, the transmissivity enlarges from 17 to 27.14%, and the jump-down point is at $I_i = 0.815$ GW/m^2, the transmittance diminishes from 30.04 to 14.06%. When $\theta = 6°$, with the strengthening of light intensity, the transmittance rises from 14.86% to 25.27% at $I_i = 1.015$ GW/m^2, and then gradually decreases. As the light strength cuts down, the transmittance descends from 35.58 to 11.95% at $I_i = 0.652$ GW/m^2. Figure 7b reveals how the transmission curve shifts with the enlargement of angle when the light is incident on the backward. When θ adds to 2°, 4°, and 6°, the upward jump points of the transmission curves are $I_i = 0.576$, 0.626, 0.739 GW/m^2, the downward jump points move to 0.24, 0.336, and 0.558 GW/m^2, and the homologous transmissivity is 49.79%, 35.25%, and 20.07%, respectively. It can be seen from the figure that no matter which direction the light is coming from, the incidence angle mainly plays a role in regulating the position and transmittance of the jump-up point.

In Fig. 8, the reflection spectral lines from the forward and backward incident light are given. When the light is from the forward, the reflectivity gradually heightens with the reinforcement of light intensity. It aggrandizes from 19.55 to 43.65% at $I_i = 1.019$ GW/m^2, and reduces from 31.37 to 17.75% at $I_i = 0.962$ GW/m^2 with a very small jump amplitude as the abatement of light intensity. When the light

is an inverted incident, the jump-up point of reflectivity is at $I_i = 0.559$ GW/m^2, and the transition range is from 10.18 to 38.98%. The jump-down point is at 0.214 GW/m^2, and the reflection index falls down from 38.87 to 8.25%.

Look at Fig. 9a, when the light is incident from the forward, as the angle adds, the shift of the jump-up point of reflectivity is very small, while the change of the jump-down point is highly obvious, so the threshold of bistable state broadens. When the angles are 2°, 4°, and 6°, the reflectivity jumps to 50.55%, 60%, and 68.93% at the jump-up position points. The jump-down point shifts to 0.905, 0.813, and 0.652 GW/m^2 in turn, and the relevant reflectivities are 35.49%, 41.7%, and 51.49%, separately. As shown in Fig. 9b, the light is incident from the backward, when the angle increases to 2°, the upward jump point of the reflectivity does not change much, but the reflectivity after the jump diminishes to 36.05% compared to 0°. The downward jump point moves to $I_i = 0.24$ GW/m^2, the reflectivity decreases from 32.24 to 8.43% as the light intensity attenuates. If the angle continues to enlarge, the reflection curves will appear to cross, so we will not continue to analyze. Observing the two pictures, the tuning effect of the angle on the reflection curves is mainly reflected in the position of the jump-down point and the maximum value of the reflectivity.

4 Conclusion

In a word, the 1D PCs' structure proposed in this paper can realize a phenomenon of non-reciprocal two-way optical bistable absorption. The simulation results show that when the light is incident from two different directions under the same conditions, the threshold interval of the ORB absorption curve will move significantly. The tuning effects of angle and magnetized plasma frequency on the ORB

absorption curves are also given. The results demonstrate that the ORB absorption produced by this structure is very sensitive to the changes of angle and magnetized plasma frequency, and adjustments to the absorption curve threshold and jump point can be achieved by slightly changing the angle and magnetized plasma frequency. Finally, we also added the reflection and transmission curves of light from the front and back incidents and the situation when their angles alter. The content of our research can be applied to the design of multifunctional devices, non-reciprocal optical isolators, optical switches, and absorbers, and the theory involved can be further applied to design the sensors.

References

1. L. Ju, X. Xie, W.C. Du, Y.J. Liu, J.J. Hao, B.L. Ma, H.W. Yang, Perfect absorption in one-dimensional photonic crystal with graphene-dielectric hyperbolic metamaterials. Phys. Status Solidi **256**, 1800382 (2018)
2. H.F. Zhang, S.B. Liu, H.M. Li, A comparative study of band Faraday effects in 3D magnetized photonic crystals with different high-symmetry lattices with uniaxial materials. J. Electromagn. Waves Appl. **28**(2), 165–183 (2013)
3. J. Ge, Y. Yin, Responsive photonic crystals. Angew. Chem. **50**(7), 1492–1522 (2011)
4. G.H. Ma, S.H. Tang, J. Shen, Z.J. Zhang, Z.Y. Hua, Defect-mode dependence of two-photon absorption enhancement in a one-dimensional photonic bandgap structure. Opt. Lett. **29**, 1769–1771 (2004)
5. G. Ma, J. Shen, Z. Zhang, Z. Hua, S.H. Tang, Ultrafast all-optical switching in one-dimensional photonic crystal with two defects. Opt. Express **14**(2), 858–865 (2006)
6. Y. Jiao, S. Fan, D.A.B. Miller, Systematic photonic crystal device design: global and local optimization and sensitivity analysis. IEEE J. Quant. Electron. **42**(3), 266–279 (2006)
7. L. Tonks, I. Langmuir, Oscillations in ionized gases. Phys. Rev. E **33**(2), 195–210 (1929)
8. V.L. Ginzburg, W.L. Sadowski, D.M. Gallik, S.C. Brown, The propagation of electromagnetic waves in plasmas. Proc. IEEE **15**(10), 70–73 (1962)
9. M. Moisan, M. Chaker, Z. Zakrzewski, J. Paraszczak, The waveguide surfatron: a high power surface-wave launcher to sustain large-diameter dense plasma columns. J. Phys. E Instr. **20**(11), 1356 (2000)
10. O. Sakai, K. Tachibana, Properties of electromagnetic wave propagation emerging in 2-d periodic plasma structures. IEEE Trans. Plasma. **35**(5), 1267–1273 (2007)
11. R. Kumar, Experimental study of electromagnetic band gaps using plasmas or defaults in a metallic photonic crystal. Microw. Opt. Technol. Lett. **53**(5), 1109–1113 (2011)
12. W.L. Fan, L. F. Dong, Dynamic control of propagating electromagnetic waves using a plasma photonic crystal. Int. Conf. Electr. Control Eng. IEEE pp. 860–863 (2010).
13. L. Song, Z. Shuangying, L. Sanqiu, A study of properties of the photonic band gap of unmagnetized plasma photonic crystal. Plasma Sci. Technol **11**(1), 14–17 (2009)
14. Y. Zhong-Cai, Impacts of collision frequency on ability of plasma to absorb the electromagnetic wave. J. Microwares **12**, 141–142 (2005)
15. W.Y. Wang, Y. Cui, Y. He, Y.R. Hao, Y.Y. Lin, X. Tian et al., Efficient multiband absorber based on one-dimensional periodic metal–dielectric photonic crystal with a reflective substrate. Opt. Lett. **39**(2), 331–334 (2014)
16. T. Fathollahi Khalkhali, B. Rezaei, A. Soltani Vala, M. Kalafi, Design of high-q polystyrene nonlinear cavity for ultrafast all-optical switching in mid-infrared photonic crystal slabs with cavity-waveguide structure. Opt. Commun. **326**, 43–47 (2014)
17. F.Y. Wang, G.X. Li, H.L. Tam, K.W. Cheah, S.N. Zhu, Optical bistability and multistability in one-dimensional periodic metal-dielectric photonic crystal. Appl. Phys. Lett. **92**(21), 211109 (2008)
18. X. Dai, L. Jiang, Y. Xiang, Low threshold optical bistability at terahertz frequencies with graphene surface plasmons. Sci. Rep. **5**(1), 12271 (2015)
19. Y. Ma, H. Zhang, T. Liu, W. Li, Study on the properties of unidirectional absorption and polarization splitting in one-dimensional plasma photonic crystals with ultra-wideband. J. Opt. Soc. Am. B **36**(8), 2250 (2019)
20. K. Arun, V. Suthar, B.K.S. Singh, P. Ojha, Nonlinear transmission and reflection characteristics of plasma/polystyrene one dimensional photonic crystal. Opt. Int. J. Light Electron Opt. **125**(1), 393–396 (2014)
21. X.K. Kong, S.B. Liu, H.F. Zhang, B.R. Bian, C. Chen, Incident angle insensitive tunable multichannel perfect absorber consisting of nonlinear plasma and matching metamaterials. Phys. Plasmas **21**(12), 207402–216155 (2014)
22. L. Qi, Z. Yang, F. Lan, X. Gao, Z. Shi, Properties of obliquely incident electromagnetic wave in one-dimensional magnetized plasma photonic crystals. Phys. Plasma **17**(4), 042501 (2010)
23. A. Kumar, V. Kumar, A. Nautiyal, K.S. Singh, S.P. Ojha, Optical switch based on nonlinear one dimensional photonic band gap material. Optik **145**, 473–478 (2017)
24. C. Li-Xue, D. Xiao-Xu, D. Wei-Qiang, Z. Yu, L. Shu-Tian, Low Threshold Bistable Switching by the Nonlinear One-Dimensional Photonic Crystal. Chin. Phys. Lett. **19**(6), 798–800 (2002)